Density-functional theory for systems of hard rods

A. Poniewierski and R. Hołyst
Institute of Physical Chemistry of the Polish Academy of Sciences, Kasprzaka 44/52, 01-224 Warsaw, Poland
(Received 30 August 1989)

We present a density-functional theory, based on the smoothed density approximation, to study systems of hard rods with full translational and orientational freedom. For hard spherocylinders, we find both the nematic-isotropic and the nematic–smectic-A transition in a wide range of length-to-width ratios $(L+D)/D$. We locate the tricritical point for the nematic–smectic-A transition and also make some predictions about the nematic–smectic-A–smectic-B point. Finally, we calculate the nematic elastic constants. The predictions of our theory are compared with the results of computer simulations and other theories. We also make some comments about application of the theory to systems of hard ellipsoids of revolution and hard cylinders.

I. INTRODUCTION

Recently there has been a revival of interest in systems of hard rods, i.e., anisotropic particles of uniaxial symmetry interacting only via hard-core repulsion. Many years ago it was shown by Onsager[1] that very long hard spherocylinders exhibit the nematic-isotropic (N-I) transition at vanishingly small densities. This means that the excluded-volume effects alone can explain orientational ordering of hard rods. On the other hand, it has been believed for a long time that formation of other liquid-crystalline phases, like smectics, cannot occur without attractive forces or flexible chains. Therefore hard rods have not been, in general, considered as a good reference system to study liquid crystals, even though it is well established that the short-range repulsive forces almost completely determine the structure of simple liquids.

At present the role of the excluded-volume effects in the formation of mesophases seems to be more appreciated. This is mainly due to the results of computer simulations carried out for hard cylinders, hard spherocylinders, and hard ellipsoids of revolution.[2–6] They provide evidence that these systems exhibit a rich variety of phase transitions observed in real liquid crystals. These results were a stimulus to new theoretical investigations[7–20] as the existing theories of dense systems of hard rods, such as the scaled particle theory[21] or the y expansion,[22,23] were not capable of reproducing rather complicated phase diagrams. Most of the present theories can be classified as density-functional theories (DFT), i.e., they treat the free energy of the system as a functional of the one-particle distribution function. In most cases they have been applied either to the N-I transition[8,9,13,23] or to systems of parallel hard rods[10,11,15,19] (see, however, Refs. 7 and 12).

Recently we have formulated a DFT for hard spherocylinders with full translational and orientational freedom,[14] in the spirit of the smoothed density approximation[24–30] (SDA). Our theory predicts both the N-I and N–Sm-A transitions in good agreement with the results of computer simulations.[6] It also provides some hints about the onset of the hexagonal order in smectic layers. As its formulation is rather general, the theory has also been applied to the N-I transition for hard cylinders and hard ellipsoids of revolution,[20] and also, after some modifications, to the N–Sm-A transition for hard parallel spherocylinders.[18]

The aim of this paper is to give more details of the calculations not presented in Ref. 14 and also to test our theory in the case of the nematic elastic constants, for which computer simulations also exist.[31]

The general theory for systems of hard rods with full translational and orientational freedom is presented in Sec. II. In Secs. III and IV we apply the theory to the N-I and N–Sm-A transitions for hard spherocylinders and also speculate about the nematic–smectic-A–smectic-B (N–Sm-A–Sm-B) point. In Sec. V we calculate the nematic elastic constants for hard spherocylinders and Sec. VI is devoted to the discussion.

II. SMOOTHED DENSITY APPROXIMATION FOR HARD RODS

The smoothed density approximation in its original form is a DFT of an inhomogeneous hard-sphere fluid.[24–30] It takes advantage of local thermodynamics but also retains the nonlocal character of the exact free-energy functional. This is achieved by introducing an auxiliary "smoothed density," which is obtained from the physical density by some weighting procedure. The free-energy functional is constructed in such a way that for a homogeneous fluid it becomes exact and also generates the exact direct correlation function. The key quantity of the SDA, the weight function, is expressed in terms of the direct correlation function for a homogeneous fluid. The SDA gives very good results both for the freezing of hard spheres and for the hard-sphere fluid near a hard wall.

Of course, the way of extension of the SDA to systems of hard rods is not unique.[15] Even for hard spheres the free-energy functional is somewhat arbitrary. To proceed in the spirit of the SDA, we refer to the local thermodynamics of a homogeneous and isotropic fluid of hard

rods and define the free-energy functional as follows:

$$F[\rho^{(1)}]=F_{\rm id}[\rho^{(1)}]+\int \rho(\mathbf{r})\Delta\psi(\bar{\rho}(\mathbf{r}))d\mathbf{r}\ , \tag{2.1}$$

where $\rho^{(1)}(\mathbf{r},\omega)$ is the one-particle distribution function depending on the position vector $\mathbf{r}$ and the orientation ω; $\rho(r)$ and $\bar{\rho}(r)$ are the physical and smoothed densities, respectively, and $\Delta\psi$ is the excess free energy per particle of the reference fluid. The ideal-gas contribution to F is given by

$$F_{\rm id}[\rho^{(1)}]=k_BT\int \rho^{(1)}(\mathbf{r},\omega)\{\ln[\Lambda^3\rho^{(1)}(\mathbf{r},\omega)]-1\}d\mathbf{r}\,d\omega\ , \tag{2.2}$$

where $1/k_BT$ is the Boltzmann factor and Λ is the thermal de Broglie wavelength. The first nontrivial step beyond the SDA for simple fluids is the relation between $\bar{\rho}$ and $\rho^{(1)}$. We use the following expression:

$$\bar{\rho}(\mathbf{r})=\int w(\mathbf{r}-\mathbf{r}',\omega,\omega';\bar{\rho}(\mathbf{r}))f(\mathbf{r},\omega)f(\mathbf{r}',\omega')\rho(\mathbf{r}') \times d\mathbf{r}'d\omega\,d\omega'\ , \tag{2.3}$$

where $f(\mathbf{r},\omega)=\rho^{(1)}(\mathbf{r},\omega)/\rho(\mathbf{r})$ is the angular distribution, $\rho(\mathbf{r})=\int\rho^{(1)}(\mathbf{r},\omega)d\omega$, and w is the weight function satisfying the normalization condition

$$\frac{1}{(4\pi)^2}\int w(\mathbf{r},\omega,\omega';\bar{\rho})d\mathbf{r}\,d\omega\,d\omega'=1\ . \tag{2.4}$$

For the isotropic fluid $f=1/4\pi$. The range of w should be related to the range of interactions. To mimic the effective reduction of interactions caused by a local orientational order, the weight function is averaged with the angular distribution. Thus

$$w_{\rm eff}(\mathbf{r},\mathbf{r}';\bar{\rho}(\mathbf{r}),[f]) =\int w(\mathbf{r}-\mathbf{r}',\omega,\omega';\bar{\rho}(\mathbf{r}))f(\mathbf{r},\omega)f(\mathbf{r}',\omega')d\omega\,d\omega' \tag{2.5}$$

can be understood as an effective weight function. Using (2.5) in (2.3) we recover the relation between $\bar{\rho}$ and ρ assumed in the SDA for simple fluids, i.e.,

$$\bar{\rho}(\mathbf{r})=\int w_{\rm eff}(\mathbf{r}-\mathbf{r}';\bar{\rho}(\mathbf{r}))\rho(\mathbf{r}')d\mathbf{r}'\ . \tag{2.6}$$

To maintain the analogy to the SDA for simple fluids, we should calculate w via the direct correlation function $c^{(2)}$ for a homogeneous and isotropic fluid of hard rods. Unfortunately, any tractable analytic form of $c^{(2)}$ for anisotropic hard bodies is not known, although there exist some numerical solutions for hard ellipsoids and spherocylinders obtained from the hypernetted chain or Percus-Yevich approximations.[32] The best we could do in this situation would be to approximate $c^{(2)}$ for hard rods using $c^{(2)}$ for hard spheres. The most popular approximation of this kind is the Pynn-Wulf approximation.[33] However, this route is not very practical because none of such approximations is reliable enough to justify the great effort put into the calculation of the weight function via $c^{(2)}$. Therefore, instead of making approximations on the level of $c^{(2)}$, we approximate the weight function itself. As a hint we have the Onsager limit of infinitely elongated hard rods. This limit is recovered if we assume that

$$w(\mathbf{r}-\mathbf{r}',\omega,\omega')=-f_2(\mathbf{r}-\mathbf{r}',\omega,\omega')/(2B_2^I) \tag{2.7}$$

together with

$$\Delta\psi(\rho)/k_BT=\rho B_2^I+[\Delta\psi^{\rm CS}(\eta)/k_BT-4\eta]\ . \tag{2.8}$$

Here f_2 is the Mayer function for hard rods,

$$B_2^I=\frac{1}{2(4\pi)^2}\int f_2(\mathbf{r},\omega,\omega')d\mathbf{r}\,d\omega\,d\omega' \tag{2.9}$$

is the second virial coefficient for a homogeneous and isotropic fluid of hard rods, $\Delta\psi^{\rm CS}(\eta)$ is the Carnahan-Starling expression for hard spheres,[34] $\eta=\rho v_0$, and v_0 is the volume of the hard rod. It is easy to check that this choice gives the proper low-density limit for $F[\rho^{(1)}]$. Our weight function is analogous to that used by Tarazona in his first formulation of the SDA.[24] Its main drawback is that it does not depend on the density. However, $w_{\rm eff}$ does depend on ρ for orientationally ordered phases due to its dependence on the angular distribution. Therefore we expect our theory to work better if the onset of a translational order occurs in an orientationally ordered system. In other words, it should describe the N–Sm-A transition better than the I–Sm-A transition. This is related to the fact that in the limit of hard spheres the weight function given by Eq. (2.7) is too simple and leads to some unphysical results.[18] We return to this point in the discussion.

Equations (2.1)–(2.9) completely determine F as a functional of $\rho^{(1)}$; thus we can express $c^{(2)}$ in terms of $\rho^{(1)}$, w, and $\Delta\psi$. For w independent of $\bar{\rho}$, it has the following form:

$$\begin{aligned}-k_BTc^{(2)}(\mathbf{r}_1,\mathbf{r}_2,\omega_1,\omega_2)=&\sum_{i=1,2}\left[\Delta\psi'(\bar{\rho}(\mathbf{r}_i))w(\mathbf{r}_1-\mathbf{r}_2,\omega_1,\omega_2)+\Delta\psi''(\bar{\rho}(\mathbf{r}_i))\Delta\bar{\rho}^{(1)}(\mathbf{r}_i,\omega_i)\int w(\mathbf{r}_1-\mathbf{r}_2,\omega_{3-i},\omega)f(\mathbf{r}_i,\omega)d\omega\right]\\&+\Delta\psi''(\bar{\rho}(\mathbf{r}_1))\Delta\bar{\rho}^{(1)}(\mathbf{r}_1,\omega_1)\Delta\bar{\rho}^{(1)}(\mathbf{r}_2,\omega_2)\delta(\mathbf{r}_1-\mathbf{r}_2)/\rho(\mathbf{r}_1)\\&+\int\rho(\mathbf{r})\Delta\psi''(\bar{\rho}(\mathbf{r}))w(\mathbf{r}_1-\mathbf{r},\omega_1,\omega)w(\mathbf{r}_2-\mathbf{r},\omega_2,\omega')f(\mathbf{r},\omega)f(\mathbf{r},\omega')d\mathbf{r}\,d\omega\,d\omega'\ ,\end{aligned} \tag{2.10}$$

where

$$\Delta\bar{\rho}^{(1)}(\mathbf{r},\omega)=\bar{\rho}^{(1)}(\mathbf{r},\omega)-\bar{\rho}(\mathbf{r}) ,$$

$$\bar{\rho}^{(1)}(\mathbf{r},\omega)=\int w(\mathbf{r}-\mathbf{r}',\omega,\omega')\rho^{(1)}(\mathbf{r}',\omega')d\mathbf{r}'d\omega' ,$$

and $\Delta\psi',\Delta\psi''$ denote, respectively, the first and second derivative with respect to $\bar{\rho}$. The term with the Dirac δ function results from the fact that $\bar{\rho}$ is not a functional of $\rho^{(1)}$ alone but depends functionally on both ρ and f. The appearance of this term is certainly a drawback of the theory. We note, however, that it vanishes in the isotropic phase and also that it contributes neither to the nematic structure factor nor to the elastic constants.

III. NEMATIC-ISOTROPIC TRANSITION

To study the *N-I* transition it is useful to have some information about the limit of stability of the isotropic phase with respect to the nematic perturbations. In general, the stability condition for F at a given stationary distribution $\rho^{(1)}(\mathbf{r},\omega)$, i.e., at which $\delta F[\rho^{(1)}]=0$, can be expressed as follows:[35]

$$\frac{\delta^2F[\rho^{(1)}]}{k_BT}=\int\frac{[\delta\rho^{(1)}(\mathbf{r},\omega)]^2}{\rho^{(1)}(\mathbf{r},\omega)}d\mathbf{r}\,d\omega-\int c^{(2)}(\mathbf{r}_1,\mathbf{r}_2,\omega_1,\omega_2)\delta\rho^{(1)}(\mathbf{r}_1,\omega_1)\delta\rho^{(1)}(\mathbf{r}_2,\omega_2)d\mathbf{r}_1d\mathbf{r}_2d\omega_1d\omega_2>0 , \tag{3.1}$$

where $\delta\rho^{(1)}$ is an arbitrary perturbation. In practice, we usually study the stability of a given solution with respect to perturbations of a particular symmetry. In the case of the nematic perturbations we have

$$\delta\rho^{(1)}=\rho\sum_{l=2,4,\ldots}f_lP_l(\cos\theta) \tag{3.2}$$

where P_l denotes the lth Legendre polynomial. Referring Eqs. (2.3) and (2.10) to the isotropic phase we find that $\bar{\rho}=\rho$, $\Delta\bar{\rho}^{(1)}=0$, and the direct correlation function is given by

$$c_I^{(2)}(\mathbf{r}_{12},\omega_1,\omega_2)=\frac{-1}{k_BT}\left[2\Delta\psi'(\rho)w(\mathbf{r}_{12},\omega_1,\omega_2)+\frac{1}{(4\pi)^2}\rho\Delta\psi''(\rho)\int w(\mathbf{r}_{12}-\mathbf{r}_3,\omega_1,\omega_3)w(\mathbf{r}_3,\omega_2,\omega_4)d\mathbf{r}_3d\omega_3d\omega_4\right] . \tag{3.3}$$

Constant perturbations, $\delta\rho^{(1)}=$const, lead to the mechanical stability condition. Combining Eqs. (3.1) and (3.3) we get

$$\delta^2F[\rho/4\pi]=(4\pi)^2\left[\frac{k_BT}{\rho}+\frac{\partial^2}{\partial\rho^2}[\rho\Delta\psi(\rho)]\right]=(4\pi)^2\frac{1}{\rho}\frac{\partial p}{\partial\rho} , \tag{3.4}$$

where p is the pressure. The condition $\partial p/\partial\rho>0$ is satisfied because of our choice of $\Delta\psi$. Substituting Eqs. (3.2) and (3.3) into Eq. (3.1) we find the stability condition for the isotropic phase with respect to the nematic perturbations:

$$\rho\sum_{l=2,4,\ldots}f_l^2\left[\frac{(4\pi)^2}{2l+1}+\frac{2\rho\Delta\psi'(\rho)}{k_BT}\int w(\mathbf{r}_{12},\omega_1,\omega_2)P_l(\omega_1)P_l(\omega_2)d\mathbf{r}_{12}d\omega_1d\omega_2\right]>0 . \tag{3.5}$$

The bifurcation density $\rho_{I\text{-}N}^*$, i.e., the smallest density at which the stability of the isotropic phase is lost, is obtained for $\delta\rho^{(1)}\propto P_2(\omega)$;[36] thus we have the following expression for $\rho_{I\text{-}N}^*$:

$$1+\frac{\rho_{I\text{-}N}^*\Delta\psi'(\rho_{I\text{-}N}^*)}{k_BT}\frac{5}{(4\pi)^2}\int w(\mathbf{r}_{12},\omega_1,\omega_2)P_2(\omega_1)P_2(\omega_2)d\mathbf{r}_{12}d\omega_1d\omega_2=0 . \tag{3.6}$$

For hard spherocylinders of length $L+D$ and diameter D, Eq. (3.6) transforms into

$$1-\frac{\rho_{I\text{-}N}^*\Delta\psi'(\rho_{I\text{-}N}^*)}{k_BT}\frac{\pi L^2D}{16B_2^I}=0 , \tag{3.7}$$

where $B_2^I=\pi D^2L+\frac{2}{3}\pi D^3+\frac{1}{4}\pi DL^2$. From Eq. (3.7) we obtain $\rho_{I\text{-}N}^*$ as a function of L/D. For $L/D=0.287$, $\rho_{I\text{-}N}^*v_0=0.784$ and is equal to the close-packing density

$$\rho_{CP}v_0=\tfrac{1}{6}\pi(3L/D+2)/(\sqrt{3}L/D+\sqrt{2}) .$$

This value of L/D can be considered as the minimal anistropy of the spherocylinder at which the bifurcation still occurs. For comparison, in the low-density approximation, the minimal anisotropy is $L/D=5.115$, which corresponds to $\rho_{I\text{-}N}^*v_0=\rho_{CP}v_0=0.884$.

To locate the *N-I* transition, we consider the free energy per particle, ψ, as a functional of the angular distribution, i.e.,

$$\psi[f]=k_BT\left[\int\ln[4\pi f(\omega)]f(\omega)d\omega+\ln(\Lambda^3\rho/4\pi)-1\right]+\Delta\psi(\bar{\rho}) . \tag{3.8}$$

We use trial functions of the Maier-Saupe form:

$$f(\omega)=\frac{\exp[\alpha P_2(\omega)]}{\int\exp[\alpha P_2(\omega')]d\omega'} \tag{3.9}$$

and minimize ψ with respect to α to find the isotropic and nematic solutions. Using Eqs. (2.3) and (2.7) we ob-

tain the following relation between $\bar{\rho}$ and ρ:

$$\bar{\rho}=\frac{\rho}{2B_2^I}\int V_0(\omega,\omega')f(\omega)f(\omega')d\omega\,d\omega' , \tag{3.10}$$

where $V_0(\omega,\omega')$ is the excluded volume. For hard spherocylinders, we find the N-I transition in the range $2.46<L/D<\infty$, while for $L/D<2.46$ a direct isotropic to smectic-A transition is expected. The orientational order parameter $Q=\langle P_2\rangle$ at the N-I transition varies from 0.56 for $L/D=2.46$ to 0.80 for $L/D=\infty$. For the density jump $\Delta\rho=2(\rho_N-\rho_I)/(\rho_N+\rho_I)$ we find $\Delta\rho=0.050$ for $L/D=2.46$ and $\Delta\rho=0.243$ for $L/D=\infty$. Thus Q and $\Delta\rho$ tend to the Onsager limit for $L/D\to\infty$, although this limit is approached rather slowly. The lines of the N-I and N–Sm-A transitions are shown in Fig. 1 and the comparison with computer simulations is presented in Sec. IV.

We have also performed calculations for hard cylinders and hard ellipsoids of revolution.[20] Both for hard spherocylinders and cylinders there exist, due to Onsager,[1] exact expressions for the excluded volume V_0. In the case of hard ellipsoids, calculations are more difficult as V_0 cannot be expressed in an analytic form. We have used the algorithm proposed by Perram and Wertheim[37] to calculate the distance of closest approach for two ellipsoids. A detailed comparison of the N-I transition for hard cylinders, spherocylinders, and ellipsoids of revolution is presented in Ref. 20. Here we only note that ellipsoids and spherocylinders give qualitatively similar results. Both systems exhibit a minimal anisotropy below which the isotropic phase is stable with respect to the nematic perturbations; for oblate ellipsoids this corresponds to the axial ratio $\sigma_\parallel/\sigma_\perp=1.35$. In the case of hard cylinders, the N-I transition persists in the whole range of elongations. For moderate elongations the transition is much more strongly first order in the case of cylinders than in the case of spherocylinders or ellipsoids. When elongations tend to infinity, we recover the Onsager limit for all three systems.

Finally, we note that our results for hard ellipsoids are in agreement both with computer simulations[4] and other theories.[9,12,23] For the axial ratio $\sigma_\parallel/\sigma_\perp=3$, we obtain $Q=0.49$, $\rho_I v_0=0.454$ (0.507), $\rho_N v_0=0.474$ (0.517), $\Delta\rho=0.043$ (0.019), and for the pressure, $pv_0/k_BT=4.68$ (9.79), where the numbers in parentheses correspond to Ref. 4.

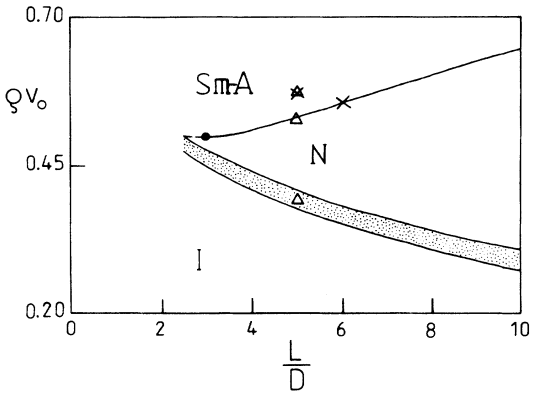

FIG. 1. Phase diagram for hard spherocylinders in the L/D-ρ plane; the shaded area corresponds to the N-I two-phase region. The dot denotes the tricritical point for the N–Sm-A transition, the triangles denote the results of computer simulations (Ref. 6) for $L/D=5$ and the crosses correspond to $\rho^*_{N\text{-Sm-}A\text{-Sm-}B}$ and $\rho^*_{\text{Sm-}A\text{-Sm-}B}$ (see text).

IV. NEMATIC–SMECTIC-A TRANSITION

It is known from computer simulations[2,3] and also from theoretical studies[10,11,15,17–19] that the system of hard parallel spherocylinders undergoes a second-order N–Sm-A transition. In this section we study hard spherocylinders with full translational and orientational freedom. Because of the coupling between translational and orientational order, a first-order N–Sm-A transition is also possible. However, if the transition occurs at a large value of the orientational order parameter, it should be continuous as for parallel spherocylinders. Therefore it is useful to study the stability limit of the nematic phase with respect to the smectic-A perturbations:

$$\delta\rho^{(1)}(\mathbf{r},\omega)=f(\omega)\delta\rho(z)=f(\omega)\sum_{n=1}^{\infty}\rho_n\cos(kz) , \tag{4.1}$$

where ρ_n is the nth smectic-A order parameter, d is the periodicity of the density wave, and $k=2\pi/d$. The stability condition (3.1) can be expressed in terms of the nematic structure factor $S_N(\mathbf{k})$ which we define as follows:

$$S_N^{-1}(\mathbf{k})=1-\rho\int e^{i\mathbf{k}\cdot\mathbf{r}}c_N^{(2)}(\mathbf{r},\omega,\omega')f(\omega)f(\omega')d\mathbf{r}\,d\omega\,d\omega' , \tag{4.2}$$

where $\mathbf{k}=k\hat{\mathbf{n}}$ is a wave vector parallel to the nematic director $\hat{\mathbf{n}}$ and $c_N^{(2)}$ is the nematic direct correlation function. Using the general expression (2.10) specified to the nematic phase, we find $S_N(\mathbf{k})$ in terms of the weight function w and the excess free energy $\Delta\psi$, i.e.,

$$S_N^{-1}(\mathbf{k})=1+\frac{\rho}{k_BT}[2\Delta\psi'(\bar{\rho})w_N(\mathbf{k})+\rho\Delta\psi''(\bar{\rho})w_N^2(\mathbf{k})] . \tag{4.3}$$

Here

$$w_N(\mathbf{k})=\int e^{i\mathbf{k}\cdot\mathbf{r}}w(\mathbf{r},\omega,\omega')f(\omega)f(\omega')d\mathbf{r}\,d\omega\,d\omega' , \tag{4.4}$$

and we have used the fact that $\int\Delta\bar{\rho}^{(1)}(\omega)f(\omega)d\omega=0$.

The nematic is stable with respect to the smectic-A perturbations if $S_N^{-1}(\mathbf{k})>0$ for all k. The loss of stability is given by the condition $S_N^{-1}(\mathbf{k})=0$ and the smallest density $\rho(\mathbf{k})$ satisfying this condition is the bifurcation density $\rho^*_{N\text{-Sm-}A}$. To find how the smectic-A solution branches off from the nematic solution, we have to express the free energy per particle in terms of the smectic order parameters. Using Eqs. (2.1)–(2.3) we find

$$\psi=F/N=k_BT\left[\ln(\Lambda^3\rho/4\pi)-1+\int\ln[4\pi f(\omega)]f(\omega)d\omega+\frac{1}{2\pi}\int_0^{2\pi}\phi(\xi)\ln\phi(\xi)d\xi\right]+\frac{1}{2\pi}\int_0^{2\pi}\phi(\xi)\Delta\psi(\rho\bar{\phi}(\xi;k,\alpha))d\xi\ , \tag{4.5}$$

where

$$\rho^{(1)}(z,\omega)=\rho f(\omega)\left[1+\sum_{n=1}^{\infty}\rho_n\cos(nkz)\right]=\rho f(\omega)\phi(kz)\ , \tag{4.6}$$

$$\bar{\phi}(\xi;k,\alpha)=w_N(0;\alpha)+\sum_{n=1}^{\infty}w_N(nk;\alpha)\rho_n\cos(n\xi)\ , \tag{4.7}$$

and α corresponds to the parametrization of the Maier-Saupe angular distribution [see Eq. (3.9)].

To determine the order of the transition, it is sufficient to leave only ρ_1 and ρ_2 in the expansion (4.6), because $\rho_n\approx\epsilon^n$ (Ref. 11) and we want to expand ψ up to ϵ^4. To facilitate the calculations, we first expand ψ in ρ_1 and ρ_2 up to the fourth order, which gives

$$\psi(\rho_1,\rho_2;\rho,\alpha,k)\cong\psi_0(\rho,\alpha)+\frac{1}{2}\left[\frac{\partial^2\psi}{\partial\rho_1^2}\right]_0\rho_1^2+\frac{1}{2}\left[\frac{\partial^2\psi}{\partial\rho_2^2}\right]_0\rho_2^2+\frac{1}{2}\left[\frac{\partial^3\psi}{\partial\rho_1^2\partial\rho_2}\right]_0\rho_1^2\rho_2+\frac{1}{4!}\left[\frac{\partial^4\psi}{\partial\rho_1^4}\right]_0\rho_1^4\ , \tag{4.8}$$

where the $(\ )_0$ corresponds to $\rho_1=\rho_2=0$ and we have included only the leading terms. All coefficients in Eq. (4.8) are functions of ρ, α, and k. The loss of stability of the nematic phase occurs at $\rho=\rho^*_{N\text{-Sm-}A}$, $\alpha=\alpha^*_{N\text{-Sm-}A}$, $k=k^*_{N\text{-Sm-}A}$ when $(\partial^2\psi/\partial\rho_1^2)_0=0$, which is equivalent to Eq. (4.3). We use the following parametrization in the neighborhood of the bifurcation point: $\rho_1=\epsilon$, $\rho_2=\frac{1}{2}\rho_2''\epsilon^2$, $\rho=\rho^*_{N\text{-Sm-}A}+\rho'\epsilon+\frac{1}{2}\rho''\epsilon^2$, $\alpha=\alpha^*_{N\text{-Sm-}A}+\alpha'\epsilon+\frac{1}{2}\alpha''\epsilon^2$, and $k=k^*_{N\text{-Sm-}A}+k'\epsilon+\frac{1}{2}k''\epsilon^2$. The last three coefficients in Eq. (4.8) couple to ϵ^4, thus they can be taken at $\epsilon=0$. The minimization of ψ with respect to ρ_2 gives the relation between ρ_2 and ρ_1, and ψ can now be expressed in terms of ϵ, α, k, and ρ as follows:

$$\psi=\psi_0(\rho,\alpha)+\frac{1}{2}\left[\frac{\partial^2\psi}{\partial\rho_1^2}\right]_0\epsilon^2+\frac{1}{4!}a^*\epsilon^4\ , \tag{4.9}$$

where

$$a^*=-3\left[\frac{\partial^3\psi}{\partial\rho_1^2\partial\rho_2}\right]^{*2}\Big/\left[\frac{\partial^2\psi}{\partial\rho_2^2}\right]^*+\left[\frac{\partial^4\psi}{\partial\rho_1^4}\right]^*$$

and the asterisk means that the derivatives are taken at the bifurcation point $\epsilon=0$. Minimizing ψ with respect to $\rho_1=\epsilon$, α, and k we obtain

$$\frac{\partial\psi}{\partial\rho_1}=\left[\frac{\partial^2\psi}{\partial\rho_1^2}\right]_0\epsilon+\tfrac{1}{6}a^*\epsilon^3=0\ , \tag{4.10}$$

$$\frac{\partial\psi}{\partial\alpha}=\left[\frac{\partial\psi}{\partial\alpha}\right]_0+\frac{1}{2}\left[\frac{\partial^3\psi}{\partial\rho_1^2\partial\alpha}\right]_0\epsilon^2=0\ , \tag{4.11}$$

$$\frac{\partial\psi}{\partial k}=\frac{1}{2}\left[\frac{\partial^3\psi}{\partial\rho_1^2\partial k}\right]_0\epsilon^2=0\ . \tag{4.12}$$

To calculate $\rho',\rho'',\alpha',\alpha''$, and k',k'', we have to differentiate Eqs. (4.10)–(4.12) with respect to ϵ at $\epsilon=0$. In zeroth order we obtain $(\partial\psi/\partial\alpha)^*=0$; the first and second derivative give, respectively, the bifurcation condition, $(\partial^2\psi/\partial\rho_1^2)^*=0$, and $(\partial^3\psi/\partial\rho_1^2\partial k)^*=0$. The final result is as follows: $\rho'=\alpha'=k'=0$ and

$$\left[\frac{\partial^2\psi}{\partial\alpha^2}\right]^*\alpha''+\left[\frac{\partial^2\psi}{\partial\alpha\,\partial\rho}\right]^*\rho''+\left[\frac{\partial^3\psi}{\partial\rho_1^2\partial\alpha}\right]^*=0\ , \tag{4.13}$$

$$\left[\frac{\partial^3\psi}{\partial\rho_1^2\partial\alpha}\right]^*\alpha''+\left[\frac{\partial^3\psi}{\partial\rho_1^2\partial\rho}\right]^*\rho''+\tfrac{1}{3}a^*=0\ , \tag{4.14}$$

$$\left[\frac{\partial^4\psi}{\partial\rho_1^2\partial k\,\partial\rho}\right]^*\rho''+\left[\frac{\partial^4\psi}{\partial\rho_1^2\partial k\,\partial\alpha}\right]^*\alpha''+\left[\frac{\partial^4\psi}{\partial\rho_1^2\partial k^2}\right]^*k''=0\ . \tag{4.15}$$

To find the difference between free energies for the smectic-A and nematic solutions, $\Delta\psi_{\text{Sm-}A-N}$, we subtract $\psi_N=\psi_0(\alpha_N(\rho),\rho)$ from ψ; $\alpha_N(\rho)$ is determined by the condition $\partial\psi_0/\partial\alpha=0$, which gives

$$\alpha_N(\epsilon)=\tfrac{1}{2}\alpha_N''\epsilon^2=-\tfrac{1}{2}\rho''\left[\frac{\partial^2\psi}{\partial\alpha\,\partial\rho}\right]^*\Big/\left[\frac{\partial^2\psi}{\partial\alpha^2}\right]^*\epsilon^2\ . \tag{4.16}$$

Using Eq. (4.9) and Eqs. (4.13)–(4.16) we arrive at the following expressions for $\Delta\psi_{\text{Sm-}A-N}$ and ρ'':

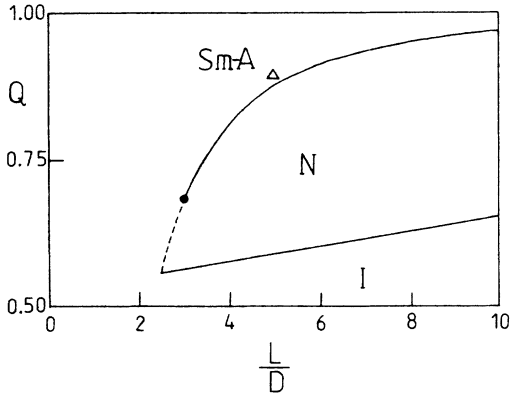

FIG. 2. Phase diagram for hard spherocylinders in the (L/D)-Q plane; meaning of symbols the same as in Fig. 1.

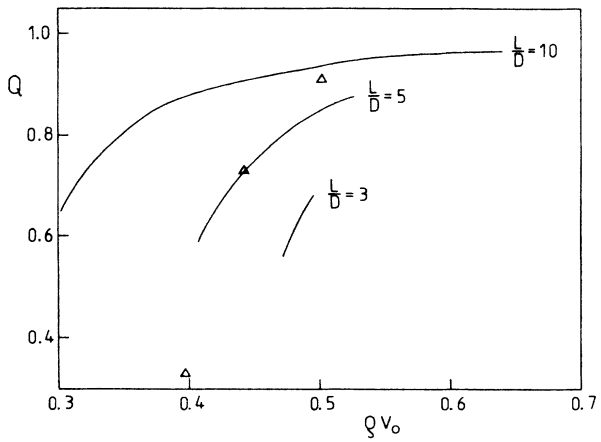

FIG. 4. Nematic order parameter vs density for $L/D=3$, 5, and 10; the triangles correspond to the computer simulations (Ref. 31).

$$\Delta\psi_{\text{Sm-}A\text{-}N} = -b^* \frac{\epsilon^4}{4!} , \tag{4.17}$$

$$\rho'' = \frac{b^*}{3} \Big/ \left[\left[\frac{\partial^2\psi}{\partial\alpha\,\partial\rho} \right]^* \left[\frac{\partial^3\psi}{\partial\rho_1^2\partial\alpha} \right]^* \Big/ \left[\frac{\partial^2\psi}{\partial\alpha^2} \right]^* - \left[\frac{\partial^3\psi}{\partial\rho_1^2\partial\rho} \right]^* \right] , \tag{4.18}$$

where

$$b^* = a^* - 3 \left[\frac{\partial^3\psi}{\partial\rho_1^2\partial\alpha} \right]^{*2} \Big/ \left[\frac{\partial^2\psi}{\partial\alpha^2} \right]^* .$$

The case $b^*>0$, in which the smectic-A solution has a lower free energy than the nematic solution, corresponds to a second-order transition; it also gives $\rho''>0$. When $b^*<0$, the smectic-A solution is unstable in some neighborhood of the bifurcation point, which indicates a first-order N–Sm-A transition. The parameter b^* depends only on the ratio L/D and we find the tricritical point, $b^*=0$, at $L/D=2.99$. We note that this value differs slightly from the value 3.29 obtained in our previous calculations[14] which contained an error. For $L/D>2.99$, b^* is positive and the N–Sm-A transition is continuous, while for $L/D<2.99$, b^* is negative and the transition is first order.

Having found the line of the second-order N–Sm-A transition, we can make a rough estimate of the N–Sm-A–Sm-B point for hard spherocylinders, i.e., the point at which the lines of the N–Sm-A, Sm-A–Sm-B, and N–Sm-B transitions meet. The smectic-B phase has a hexagonal order in layers and we can assume, in the first approximation, that the crystallization in layers is similar to the crystallization of two-dimensional hard disks of diameter D, which occurs at the surface density $\rho_s^{\text{HD}}\pi(D/2)^2=0.69$.[38] This assumption is reasonable if the orientational order parameter is sufficiently high. To

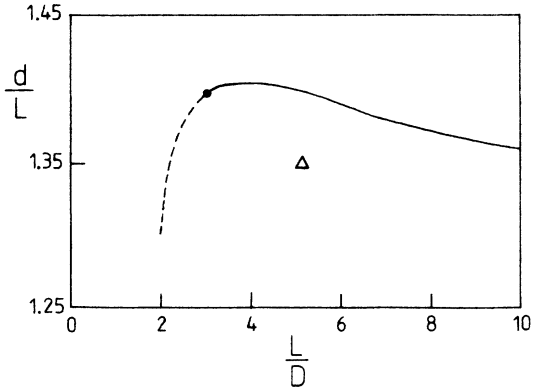

FIG. 3. Periodicity of the density wave vs L/D at the N–Sm-A bifurcation; meaning of symbols the same as in Fig. 1.

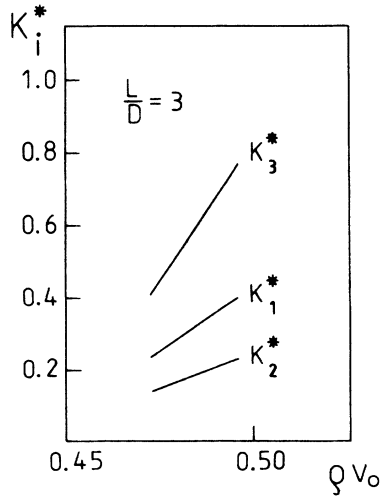

FIG. 5. Elastic constants vs density for $L/D=3$.

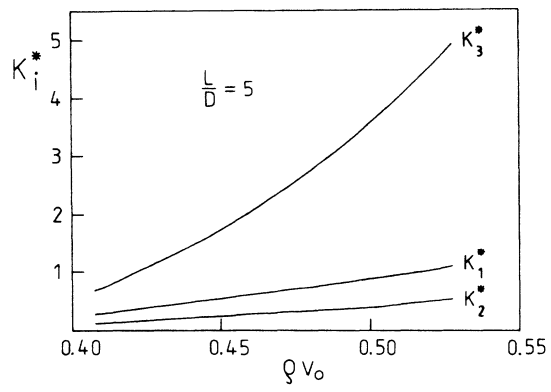

FIG. 6. Elastic constants vs density for $L/D=5$.

translate ρ_s into a three-dimensional density, we use the following expression:

$$\rho v_0=\frac{\rho_s v_0}{d}=\rho_s\pi\left[\frac{D}{2}\right]^2\frac{L}{d}\left[1+\frac{2}{3}\frac{D}{L}\right]. \tag{4.19}$$

Substituting in Eq. (4.19) $\rho=\rho^*_{N\text{-Sm-}A}(L/D)$ and $\rho_s=\rho_s^{\mathrm{HD}}$, we find that the equation is satisfied for $L/D\cong 6$ and $\rho^*_{N\text{-Sm-}A}v_0\cong 0.55$, $d/L\cong 1.39$, and $Q\cong 0.91$. We can also use Eq. (4.19) to estimate the density $\rho^*_{\text{Sm-}A\text{-Sm-}B}$ at which, for a given value of L/D, the onset of the hexagonal ordering in smectic layers can be expected. In this case we simply take $\rho_s=\rho_s^{\mathrm{HD}}$ and approximate $d=d(L/D)$ by the value obtained for the N-Sm-A bifurcation (see Fig. 3), to find that $\rho^*_{\text{Sm-}A\text{-Sm-}B}=0.56$ at $L/D=5$.

In Fig. 1 we present the isotropic ρ_I and the nematic ρ_N densities at the N-I transition and $\rho^*_{N\text{-Sm-}A}$ at the N-Sm-A bifurcation, for L/D between 2.46 and 10. The densities ρ_N and $\rho^*_{N\text{-Sm-}A}$ have the same value at $L/D=2.46$. Because the first-order N-Sm-A transition occurs at a nematic density smaller than the bifurcation density, the N-I-Sm-A triple point should be at L/D slightly above 2.46. The tricritical point for the N-Sm-A transition occurs at $L/D=2.99$. The cross on the line of the continuous N-Sm-A transition denotes the N-Sm-A-Sm-B point and the other cross, at $L/D=5$, denotes the density at which the onset of the smectic-B ordering should occur. The triangles show, in increasing sequence, the densities ρ_I, $\rho^*_{N\text{-Sm-}A}$, and $\rho^*_{\text{Sm-}A\text{-Sm-}B}$ obtained from computer simulations[6] for $L/D=5$. In Fig. 2 we plot Q versus L/D at the N-I transition and the N-Sm-A bifurcation, and the periodicity of the smectic-A at the N-Sm-A bifurcation versus L/D is plotted in Fig. 3. We note that the sharp decrease of d occurs for L/D below the tricritical point; thus it does not correspond to the N-Sm-A transition, which is first order, but only to the N-Sm-A bifurcation. The comparison with the computer simulations for $L/D=5$ (Ref. 6) is as follows.

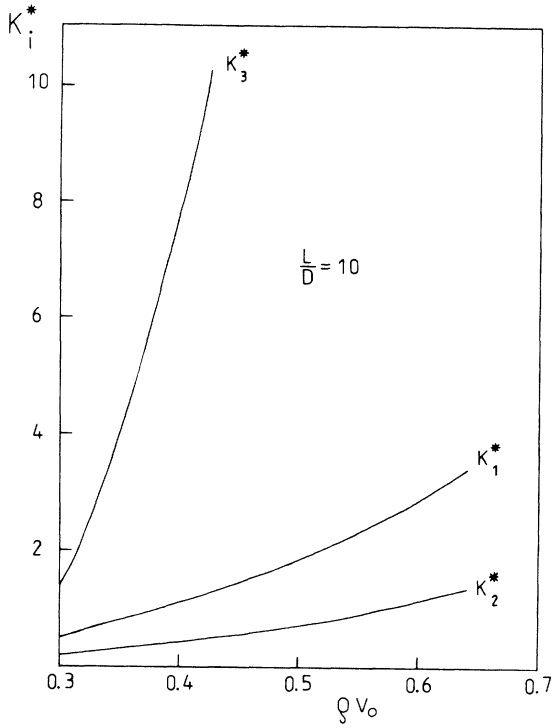

FIG. 7. Elastic constants vs density for $L/D=10$.

TABLE I. Elastic constants for hard spherocylinders with $L/D=5$ at two densities. For comparison, the results obtained from the computer simulations and theory of Sin-Doo Lee are presented.

Source	ρ/ρ_{CP}	Q	K_1^*	K_2^*	K_3^*
Reference 31[a]	0.500	0.73	0.83±0.11	0.59±0.03	1.10±0.05
	0.569	0.91	4.64±0.26	2.25±0.09	1.51±0.14
Reference 43	0.482	0.729	1.322	0.441	6.447
	0.566	0.905	2.985	0.995	38.67
Present work	0.500	0.728	0.513	0.239	1.526
	0.569	0.849	0.907	0.430	3.705

[a]All values of the elastic constants in Ref. 31 should be multiplied by $\frac{9}{4}$ (Ref. 44); we present the corrected numbers.

(1) The N-I transition: $Q=0.59$ (0.3), $\rho_I v_0=0.38$ (0.40), $\rho_N v_0=0.41$.

(2) The N–Sm-A transition, $Q=0.88$ (0.9), $\rho^*_{N\text{-Sm-}A}=0.53$ (0.53), $d/L=1.40$ (1.35).

(3) $\rho^*_{\text{Sm-}A\text{-Sm-}B}=0.56$ (0.57).

The numbers in parentheses have been taken from Ref. 6.

Finally, we calculate the average deviation of the spherocylinder from the ideal alignment, defined as $x=L\langle\sin\theta\rangle$, along the line of the continuous N–Sm-A transition. We find that x/D varies from 1.26 for $L/D=4$ to 1.32 for $L/D=10$, thus it is almost constant at the N–Sm-A transition. This means that x/D must be sufficiently small for the N–Sm-A transition to occur. Therefore Q at the transition increases with L/D and is close to unity for long spherocylinders. However, in the absence of external ordering fields, a high degree of alignment can be achieved only by the increase of the density, which explains why $\rho^*_{N\text{-Sm-}A}$ increases with L/D.

V. NEMATIC ELASTIC CONSTANTS

The nematic elastic constants, or Frank elastic constants, appear in the free energy of deformation F_d of the nematic liquid crystal.[39] F_d can be expressed in terms of three invariants involving gradients of the nematic director field $\hat{\mathbf{n}}(r)$ as follows:

$$F_d=\tfrac{1}{2}\int[K_1(\mathrm{div}\hat{\mathbf{n}})^2+K_2(\hat{\mathbf{n}}\cdot\mathrm{rot}\hat{\mathbf{n}})^2+K_3(\hat{\mathbf{n}}\times\mathrm{rot}\hat{\mathbf{n}})^2]d\mathbf{r}\ , \tag{5.1}$$

where K_1,K_2,K_3 are the elastic constants corresponding to the "splay," "twist," and "bend" deformations, respectively. To calculate the elastic constants for the SDA, we use the microscopic expressions derived in Ref. 40, i.e.,

$$K_1=-\tfrac{1}{2}k_BT\rho^2\int x^2c_N^{(2)}(\mathbf{r},\hat{\boldsymbol{\omega}}_1,\hat{\boldsymbol{\omega}}_2)\omega_{1x}\omega_{2x}f'(\cos\theta_1)f'(\cos\theta_2)d\mathbf{r}\,d\hat{\boldsymbol{\omega}}_1d\hat{\boldsymbol{\omega}}_2\ , \tag{5.2}$$

$$K_2=-\tfrac{1}{2}k_BT\rho^2\int x^2c_N^{(2)}(\mathbf{r},\hat{\boldsymbol{\omega}}_1,\hat{\boldsymbol{\omega}}_2)\omega_{1y}\omega_{2y}f'(\cos\theta_1)f'(\cos\theta_2)d\mathbf{r}\,d\hat{\boldsymbol{\omega}}_1d\hat{\boldsymbol{\omega}}_2\ , \tag{5.3}$$

$$K_3=-\tfrac{1}{2}k_BT\rho^2\int z^2c_N^{(2)}(\mathbf{r},\hat{\boldsymbol{\omega}}_1,\hat{\boldsymbol{\omega}}_2)\omega_{1x}\omega_{2x}f'(\cos\theta_1)f'(\cos\theta_2)d\mathbf{r}\,d\hat{\boldsymbol{\omega}}_1d\hat{\boldsymbol{\omega}}_2\ , \tag{5.4}$$

where the z axis is parallel to the nematic director, $\hat{\boldsymbol{\omega}}_i=(\sin\theta_i\cos\phi_i,\sin\theta_i\sin\phi_i,\cos\theta_i)$, $i=1,2$, and f' denotes the derivative of the angular distribution. Using Eq. (2.10) we find that $c_N^{(2)}=-2\Delta\psi'(\bar{\rho})w/k_BT+$(other terms). Because of the selection rules, these other terms do not contribute to the elastic constants. Thus, for a given f, the SDA gives the same proportions between the elastic constants as the low-density approximation $c_N^{(2)}\cong f_2$.

We have carried out calculations of the elastic constants for hard spherocylinders with $L/D=3$, 5, and 10, using the Maier-Saupe form of $f(\cos\theta)$. The dependence of the nematic order parameter on the density, in the range of densities between the N-I and the N–Sm-A transitions, is shown in Fig. 4. The triangles denote the results of the computer simulations[31] for $L/D=5$ and for $\rho/\rho_{CP}=0.45$, 0.5, and 0.569 where $\rho_{CP}v_0=0.8835$ is the close-packing density. In our theory the density $\rho=0.45\rho_{CP}$ is slightly below the nematic density at the N-I transition. In Figs. 5–7 we present the dimensionless elastic constants $K_i^*=K_iD/k_BT$ as functions of the density, for $L/D=3,5,10$, respectively. The range of the densities is the same as in Fig. 4.

Recently there have been several papers concerning the density-functional approach to the nematic elastic constants.[41–43] In Table I we compare our results for hard spherocylinders with the computer simulations of Allen and Frenkel[31] and also with the theory of Sin-Doo Lee.[43] In the case of $\rho/\rho_{CP}=0.5$, the agreement of our theory with the simulations is reasonably good. For $\rho/\rho_{CP}=0.569$, our K_1 and K_2 are too small but we note that also Q is smaller than in the simulations. Both theories overestimate the value of K_3, although our results are closer to the results of simulations. However, the results of simulations for K_3 are the least certain as it is pointed out in Ref. 31.

VI. DISCUSSION

We have presented a density-functional theory that is a simple extension of the smoothed density approximation to systems of anisotropic hard bodies. The theory has been applied to hard spherocylinders with full translational and orientational freedom and tested in the following three cases: (1) the nematic-isotropic transition, (2) the nematic–smectic-A transition, and (3) the nematic elastic constants. In all cases we obtain qualitatively correct results. Also the quantitative agreement with available computer simulations is reasonably good. For sufficiently anisotropic spherocylinders our theory predicts both the N-I and N–Sm-A transitions. The former is always a first-order transition, whereas the latter can be either first or second order depending on the ratio L/D. For less anisotropic spherocylinders a direct I–Sm-A transition should occur but this has not been studied numerically. There are also some indications that our theory should predict the Sm-A–Sm-B transition. We have roughly estimated the location of the N–Sm-A–Sm-B point and the location of the Sm-A–Sm-B transition for $L/D=5$. The latter compares well with the result of the computer simulations.

It is interesting to compare the simulations for parallel spherocylinders[3] with the simulations for freely rotating spherocylinders.[6] In the former case a first-order

smectic-A-columnar transition is found, while in the latter, there are indications that the Sm-A–Sm-B transition occurs. In both cases, for $L/D=5$, the density of the smectic-A at the transition is around 61–65% of the close-packing density. To have some idea how the full phase diagram for freely rotating spherocylinders may look, we superimpose the line of the N–Sm-A transition, obtained from our theory, on the phase diagram for parallel spherocylinders, obtained from the simulations.[3] This line crosses the two-phase region for the smectic-A-columnar transition. This suggests two possible scenarios.

(1) The line of the N–Sm-A transition terminates at this two-phase region but instead of the columnar phase we rather expect the smectic-B phase.

(2) The line of the N–Sm-A transition has its "echo" on the other side of this two-phase region, which separates the low-density columnar phase from the high-density smectic-B phase. In this case we would have the following transitions: $N\rightarrow$Sm-$A\rightarrow$Sm-B for $L/D<6$, $N\rightarrow$Sm-B for $6<L/D<(L/D)_{\rm col}$, and $N\rightarrow$columnar $\rightarrow$Sm-B for $(L/D)_{\rm col}<L/D$, where $(L/D)_{\rm col}$ denotes the lower bound of the region in which the columnar phase would exist.

Whether one of these pictures is correct cannot be answered until more computer simulations, especially for $L/D\geq 6$, are available. However, some hints can be provided by studies of phase transitions in dispersions of rodlike colloidal particles.[45–48]

The main drawback of the theory is that it is rather limited to sufficiently anisotropic spherocylinders for the following reasons. Our theory is based on the low-density approximation for the weight function, which is well justified in the limit of $L/D\rightarrow\infty$. However, in the opposite hard-sphere limit ($L/D=0$) this approximation is rather poor and results in a divergence of the structure factor $S(\mathbf{k})$ before crystallization of hard spheres.[18] The remedy for this would be the addition to our weight function of the density-dependent part of the weight function for hard spheres, i.e., $\Delta w^{\rm HS}=w^{\rm HS}(r,\rho)-3f_2^{\rm HS}(r)/(4\pi\sigma^3)$, in the form given by Tarazona[25] or Curtin and Ashcroft.[26] We believe that the unphysical predictions of the theory for small L/D do not influence our results for the N–Sm-A transition, which occurs for $L/D\gg 1$. This is because the rotational symmetry of the system has already been broken and the translational order appears in the system of aligned spherocylinders. On a more technical level, this means that the effective weight function depends on the density through the angular distribution.

In the case of the nematic elastic constants, the agreement of our theory with computer simulations is worse than in the case of the N-I and N–Sm-A phase transitions. This is not surprising because the elastic constants are rather sensitive to the details of the direct correlation function and also the angular distribution.[41] There is also another factor which may be important, namely, the symmetry of $c^{(2)}$. Usually it is assumed that $c^{(2)}$ has the full rotational symmetry even in the nematic phase. The proper nematic symmetry of $c^{(2)}$ can be taken into account by the inclusion of higher-order direct correlation functions for the isotropic phase.[42] Our free-energy functional does generate an anisotropic $c^{(2)}$ but this anisotropy does not appear in the final expressions for K_i, which is also a drawback of our theory.

Finally, we note that our version of the SDA applied to the N-I transition resembles the modified weighted-density approximation (MWDA), formulated recently by Denton and Ashcroft[49] for nonuniform simple liquids.

We conclude that density-functional theories based on the SDA give promising results also in the case of hard anisotropic bodies, even though a more formal justification of the SDA both for hard spheres and hard rods is necessary.

ACKNOWLEDGMENTS

We would like to thank Professor J. Stecki for his constant interest and for the critical reading of this manuscript. We are also grateful to Professor D. Frenkel for helpful discussions. This work has been carried out under the Research Project, Centralny Program Badań Podstawowych 01.12.12.1.

[1] L. Onsager, Ann. N.Y. Acad. Sci. **51**, 627 (1949).
[2] A. Stroobants, H. N. W. Lekkerkerker, and D. Frenkel, Phys. Rev. Lett. **57**, 1452 (1986).
[3] A. Stroobants, H. N. W. Lekkerkerker, and D. Frenkel, Phys. Rev. A **36**, 2929 (1987).
[4] D. Frenkel and B. M. Mulder, Mol. Phys. **55**, 1171 (1985).
[5] D. Frenkel, Mol. Phys. **60**, 1 (1987).
[6] D. Frenkel, J. Phys. Chem. **92**, 3280 (1988).
[7] U. P. Singh and Y. Singh, Phys. Rev. A **33**, 2725 (1986).
[8] Sin-Doo Lee, J. Chem. Phys. **87**, 4972 (1987); **89**, 7036 (1988).
[9] M. Baus, J. L. Colot, X. G. Wu, and H. Xu, Phys. Rev. Lett. **59**, 2184 (1987).
[10] X. Wen and R. B. Meyer, Phys. Rev. Lett. **59**, 1325 (1987).
[11] B. Mulder, Phys. Rev. A **35**, 3095 (1987).
[12] J. F. Marko, Phys. Rev. Lett. **60**, 325 (1988).
[13] J. L. Colot, X. G. Wu, H. Xu, and M. Baus, Phys. Rev. A **38**, 2022 (1988).
[14] A. Poniewierski and R. Hołyst, Phys. Rev. Lett. **61**, 2461 (1988).
[15] A. M. Somoza and P. Tarazona, Phys. Rev. Lett. **61**, 2566 (1988).
[16] L. Mederos and D. E. Sullivan, Phys. Rev. A **39**, 854 (1989).
[17] M. P. Taylor, R. Hentschke, and J. Herzfeld, Phys. Rev. Lett. **62**, 800 (1989).
[18] R. Hołyst and A. Poniewierski, Phys. Rev. A **39**, 2742 (1989).
[19] J. M. Caillol and J. J. Weis, J. Chem. Phys. **90**, 7403 (1989).
[20] R. Hołyst and A. Poniewierski, Mol. Phys. **68**, 381 (1989).
[21] M. A. Cotter and D. E. Martire, J. Chem. Phys. **52**, 1902 (1970); **52**, 1909 (1970); M. A. Cotter, Phys. Rev. A **10**, 625 (1974); and J. Chem. Phys. **66**, 1098 (1977).
[22] B. Barboy and W. M. Gelbart, J. Chem. Phys. **71**, 3035 (1979); J. Stat. Phys. **22**, 685 (1980); **22**, 709 (1980).
[23] B. M. Mulder and D. Frenkel, Mol. Phys. **55**, 1193 (1985).
[24] P. Tarazona, Mol. Phys. **52**, 81 (1984); P. Tarazona and R.

Evans, *ibid.* **52**, 847 (1984).
[25]P. Tarazona, Phys. Rev. A **31**, 2672 (1985).
[26]W. A. Curtin and N. W. Ashcroft, Phys. Rev. A **32**, 2909 (1985).
[27]W. A. Curtin and N. W. Ashcroft, Phys. Rev. Lett. **56**, 2775 (1986).
[28]W. A. Curtin, Phys. Rev. Lett. **59**, 1228 (1987).
[29]T. F. Meister and D. M. Kroll, Phys. Rev. A **31**, 4055 (1985).
[30]R. D. Groot and J. P. van der Eerden, Phys. Rev. A **36**, 4356 (1987).
[31]M. P. Allen and D. Frenkel, Phys. Rev. A **37**, 1813 (1988).
[32]A. Perera, P. G. Kusalik, and G. N. Patey, J. Chem. Phys. **87**, 1295 (1987); **89**, 5969 (1989); A. Perera and G. N. Patey, *ibid.* **89**, 5861 (1988).
[33]R. Pynn, Solid State Commun. **14**, 29 (1974); A. Wulf, J. Chem. Phys. **67**, 2254 (1977).
[34]N. F. Carnahan and K. E. Starling, J. Chem. Phys. **51**, 635 (1969).
[35]J. Stecki and A. Kloczkowski, J. Phys. (Paris) Colloq. **40**, C3-360 (1979); Mol. Phys. **42**, 51 (1981).
[36]R. F. Kayser, Jr. and H. J. Raveché, Phys. Rev. A **17**, 2067 (1978); K. Lipszyc and A. Kloczkowski, Acta Phys. Pol. A **63**, 805 (1983).
[37]J. W. Perram and M. S. Wertheim, J. Comput. Phys. **58**, 409 (1985).
[38]F. H. Ree, in *Physical Chemistry, An Advanced Treatise,* edited by H. Eyring, D. Henderson, and W. Jost (Academic, New York, 1971), Vol. 8A, Chap. 3.
[39]F. C. Frank, Discuss. Faraday Soc. **25**, 19 (1958).
[40]A. Poniewierski and J. Stecki, Mol. Phys. **38**, 1931 (1979); Phys. Rev. A **25**, 2368 (1982).
[41]Sin-Doo Lee and R. B. Meyer, J. Chem. Phys. **84**, 3443 (1986).
[42]Y. Singh and K. Singh, Phys. Rev. A **33**, 3481 (1986); K. Singh and Y. Singh, *ibid.* **34**, 548 (1986).
[43]Sin-Doo Lee, Phys. Rev. A **39**, 3631 (1989).
[44]D. Frenkel (private communication).
[45]J. A. N. Zasadzinsky, M. J. Sammon, R. E. Meyer, M. Cahoom, and D. L. D. Caspar, Mol. Cryst. Liq. Cryst. **138**, 211 (1986).
[46]F. P. Booy and A. G. Fowler, Int. J. Biol. Macromol. **7**, 327 (1985).
[47]H. N. W. Lekkerkerker, in *Phase Transitions in Soft Condensed Matter,* edited by T. Riste and D. Sherington (Plenum, New York, in press).
[48]X. Wen, R. B. Meyer, and D. L. D. Caspar, Phys. Rev. Lett. **63**, 2760 (1989).
[49]A. R. Denton and N. W. Ashcroft, Phys. Rev. A **39**, 4701 (1989).